JOURNAL OF AIRCRAFT
Vol. 43, No. 5, September–October 2006

Icing Encounter Flight Simulator

Robert W. Deters,* Glen A. Dimock,† and Michael S. Selig‡
University of Illinois at Urbana–Champaign, Urbana, Illinois 61801

DOI: 10.2514/1.20364

The Icing Encounter Flight Simulator is one part of the Smart Icing Systems project at the University of Illinois at Urbana–Champaign. From the Smart Icing Systems project, an ice management system was designed that would sense and characterize ice, notify the pilot, and if necessary take measures to ensure the safety of the aircraft. The icing simulator was used as a platform to integrate and test different components of the Smart Icing System. To create an Icing Encounter Flight Simulator, functionality and Smart Icing System components were added to the FlightGear flight simulator. Functionality added to FlightGear include a reconfigurable aircraft model and an icing model, and Smart Icing System components added include an envelope protection system and a glass cockpit enhanced with ice management system features. To ensure a real-time simulation, computationally intensive processes were distributed over several desktop computers linked together through a local network. In order to demonstrate the effectiveness of the Smart Icing System components, two fictional but historically motivated icing scenarios were developed and tested with a simulated DeHavilland DHC-6 Twin Otter, specifically, a tailplane stall event during a steep descent and a roll upset event during an emergency approach.

Introduction

As part of the Smart Icing Systems (SIS) project [1,2] at the University of Illinois at Urbana–Champaign, the Icing Encounter Flight Simulator (IEFS) [3–5] integrates various SIS components in a simulated aircraft icing environment. The SIS project was started to investigate measures that would help keep the aircraft safe during an icing encounter. To do this an ice management system (IMS) was devised that would sense and characterize the presence of ice, notify the pilot, and ensure the safety of the aircraft. To test and demonstrate the IMS, the IEFS was designed to integrate the different aspects of the SIS project such as the flight dynamics model, autopilot [6], aircraft icing model [7,8], icing characterization routine [9], envelope protection system (EPS) [10], and human factors [11].

Instead of creating a new flight simulator for this project, it was decided to adapt an existing simulator. The simulator chosen was the FlightGear flight simulator (FGFS)[§] for its open source and modular code. Added to FlightGear were a reconfigurable aircraft model, autopilot, and an icing model. Other aspects of the SIS such as the ice weather model, EPS, ice protection system (IPS), neural-network-based icing characterization, and the IMS-enhanced glass cockpit were integrated into the IEFS. Several components of the IEFS became too computationally intensive to run on a single desktop PC, and so to ensure real-time simulations, the IEFS was divided into different modules to be run over a local area network. The resulting distributed simulator contains six modules: flight dynamics model (FlightGear with the autopilot and icing model), SIS support code (ice weather model, EPS, and IPS), neural-network-based icing characterization, IMS-enhanced glass cockpit, simulation state server, and out-the-window views from Microsoft Flight Simulator 2002.

Testing and demonstrating the IEFS was accomplished through two icing scenarios: tailplane stall and roll upset. The scenarios consider a 40-passenger aircraft, but flight dynamics are modeled after the twin turboprop DHC-6 Twin Otter. The Twin Otter flight model was used due to the extensive body of icing data available for this aircraft and because NASA has historically used it in icing research. Tailplane stall occurs when ice on the horizontal stabilizer causes an uncommanded pitch down maneuver. Roll upset occurs when wing ice leads to flow separation near the ailerons causing an uncommanded rolling moment. These scenarios are fictional but based on historical factors that have led to icing events.

Background

SIS Project

The SIS [1,2] project with funding funded principally through NASA Glenn was started to develop a system that would sense the presence of in-flight ice and its effects, notify the pilot, and if necessary take measures to secure the safety of the aircraft in the icing conditions. The SIS project itself is multidisciplinary combining the areas of aerodynamics and propulsion, flight mechanics, controls and sensor integration, human factors and cognitive engineering, and aircraft icing technology (Fig. 1). A key functional outcome of the joint effort work is an IMS designed to 1) sense the presence of and characterize the effects of ice accretion on the aircraft, 2) manage the IPS and if necessary automatically activate it, and 3) modify the EPS to ensure that the aircraft stays in a safe flight envelope. During each function of the IMS, the pilot is kept informed of all relevant information. The SIS project also included flight simulation and flight tests for model verification and integration.

The purpose of the IMS is to provide another layer of safety during an icing encounter. It is designed not to replace the IPS of an aircraft but instead work with the IPS. A graphical representation of how an icing accident can occur is conceptually illustrated in Fig. 2 (adapted from Maurino et al. [12]). An aircraft with just an IPS has three layers of defense against an icing event. Each layer has gaps in protection (represented by holes), and in the unlikely event that the gaps of each layer line up, an icing accident is possible. Aircraft with an IMS have an added layer of protection to decrease the likelihood of an accident. Even the IMS is not foolproof, and it too is represented with gaps.

To tackle the complicated problem of designing and testing the IMS, the SIS project was divided into several smaller groups: aerodynamics and flight mechanics, icing characterization, autopilot and envelope protection, flight deck displays and human factors, and flight simulation. Aerodynamics and flight mechanics developed the aircraft and icing models and verified the models against flight test data. The icing characterization group developed a neural-network-based icing characterization routine to sense the presence of ice accretion and determine its effects on the aircraft. The autopilot and

Presented as Paper 0817 at the 40th AIAA Aerospace Sciences Meeting and Exhibit, Reno, NV, 14–17 January 2002; received 4 October 2005; revision received 13 February 2006; accepted for publication 15 February 2006.

*Graduate Research Assistant; rdeters@uiuc.edu. Student Member AIAA.
†Graduate Research Assistant; dimock@gmail.com. Student Member AIAA.
‡Associate Professor; m-selig@uiuc.edu. Senior Member AIAA.

§Data available on-line at http://www.flightgear.org [cited 3 January 2006].

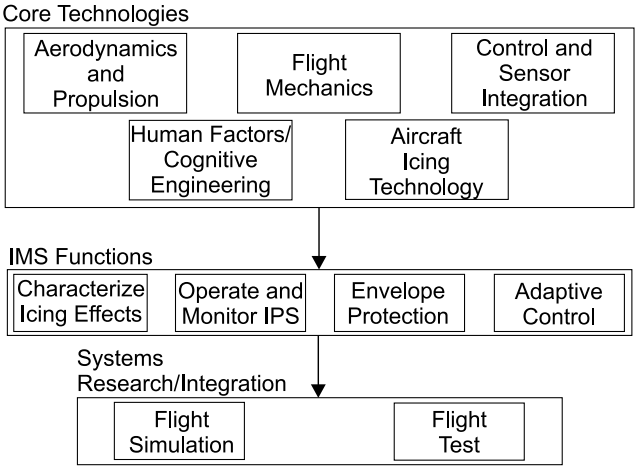

Fig. 1 SIS research group organization.

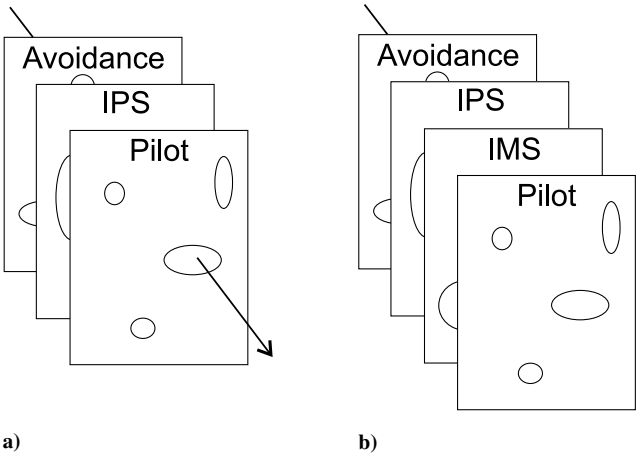

a) **b)**

Fig. 2 Layers of defense against an icing event. a) Aircraft without an IMS, and an icing incident is shown by the arrow through the layers of defense. b) Aircraft with an IMS. This new layer stops the incident from occurring.

envelope protection group is self-explanatory. The flight deck display and human factors group designed an IMS-enhanced glass cockpit to effectively display relevant data to the pilot. The flight simulation group (the authors) served as system integrators in creating a simulator that combined all of the parts of the IMS and provided a testing platform.

FGFS Project

The flight dynamics model of the Icing Encounter Flight Simulator is based on the FlightGear flight simulator. FGFS is an open source multiplatform flight simulator written in C/C++ and employs OpenGL for its graphics. FlightGear is open source and adheres to the GNU General Public License (GPL), which allows anyone to modify and redistribute the code.[‖]

In 1999, the University of Illinois at Urbana–Champaign (UIUC) Smart Icing Systems Research Group started to adapt FlightGear for its own purposes. The SIS group developed a reconfigurable aircraft model to work with the LaRCsim flight dynamics model (FDM), a workstation-based flight simulator developed by Jackson of NASA Langley [13] that was already incorporated into FlightGear. Along with the reconfigurable aircraft model, an icing model was incorporated, and the ability to fly icing scenarios was added. On May 18, 2000, the first version of FlightGear to include the UIUC model was released.

[‖]"GNU General Public License," 2003, data available on-line at http://www.gnu.org/copyleft/gpl.html [cited 3 January 2006].

IEFS Development

To create an Icing Encounter Flight Simulator, new functionality was added to FlightGear and components were integrated into the IEFS. The first step was the creation of a reconfigurable aircraft model that uses the flight dynamics model of LaRCsim. This reconfigurable aircraft model uses a keyword-based input file to describe the properties of the aircraft, such as geometry, mass, aerodynamic model, engine model, gear model, icing model, and initial conditions. Also included is the ability to set flags on what variables are to be saved to an output file for postprocessing. There are over 370 keywords to define the aircraft properties and over 400 recordable variables. With the aircraft properties, the forces and moments acting on the aircraft are calculated and the LaRCsim module determines the next aircraft state. Figure 3 shows a conceptual representation of the reconfigurable aircraft model.

Elements of the reconfigurable aircraft model discussed are the aerodynamics model, autopilot, and simulator batch mode. Three SIS components were also integrated into the simulator: icing model, ice management system, and IMS-enhanced glass cockpit. The icing model modifies the aerodynamic characteristics of the aircraft to simulate ice accretion, the IMS characterizes the ice and ensures the safety of the aircraft through the IPS and EPS, and the glass cockpit provides the pilot with icing related data. The main processes of the IMS are divided among different components. Sensing ice accretion is performed by a neural-network-based icing characterization routine. Characterizing the effects of the ice accretion is accomplished by the neural network and by an envelope protection system that also detects unsafe maneuvers [2]. Protection of the aircraft is fulfilled by an ice protection system along with the EPS. A more detailed discussion of the reconfigurable aircraft model and SIS components can be found in the Master's Thesis by Deters [14].

Aerodynamics Model

Aerodynamic data are specified using the reconfigurable aircraft model by two methods. Data are provided in the form of linear stability and control derivatives or in the form of lookup tables. Specifying aerodynamic data are done by exclusively using linear stability and control derivatives, exclusively using lookup tables, or using a combination of the two. While using linear stability and control derivatives or lookup tables, aerodynamic data are supplied in the wind-axis system or the body-axis system. The advantage of the lookup tables is that nonlinear data can be provided. These lookup tables are provided to the simulator in the form of data files that are read in and stored during initialization. The tables can be one, two, or three dimensional.

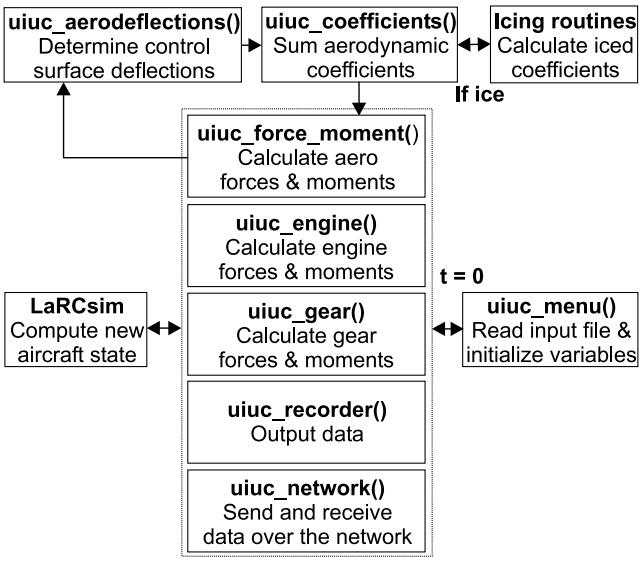

Fig. 3 Conceptual overview of the UIUC model.

Two Twin Otter aerodynamic models are used with the IEFS. The first model uses linear stability and control derivatives based on the body-axis system calculated from published NASA Twin Otter flight results [2]. The three aerodynamic force coefficients and the three aerodynamic moment coefficients are calculated by

$$C_Z = C_{Z_0} + C_{Z_\alpha}\alpha + C_{Z_{\delta_e}}\delta_e + C_{Z_q} q \frac{\bar{c}}{2V} \tag{1}$$

$$C_X = C_{X_0} + C_{X_\alpha}\alpha + C_{X_{\alpha^2}}\alpha^2 \tag{2}$$

$$C_m = C_{m_0} + C_{m_\alpha}\alpha + C_{m_{\delta_e}}\delta_e + C_{m_q} q \frac{\bar{c}}{2V} \tag{3}$$

$$C_Y = C_{Y_\beta}\beta + C_{Y_{\delta_r}}\delta_r + C_{Y_p} p \frac{b}{2V} + C_{Y_r} r \frac{b}{2V} \tag{4}$$

$$C_l = C_{l_\beta}\beta + C_{l_{\delta_a}}\delta_a + C_{l_{\delta_r}}\delta_r + C_{l_p} p \frac{b}{2V} + C_{l_r} r \frac{b}{2V} \tag{5}$$

$$C_n = C_{n_\beta}\beta + C_{n_{\delta_a}}\delta_a + C_{n_{\delta_r}}\delta_r + C_{n_p} p \frac{b}{2V} + C_{n_r} r \frac{b}{2V} \tag{6}$$

The second model uses a series of 24 three-dimensional lookup tables to model the nonlinear aerodynamics of the Twin Otter based on wind tunnel tests performed by Bihrle Applied Research, Inc. There are six sets of lookup tables corresponding to the three aerodynamic force coefficients acting along the body-axis system (C_x, C_y, C_z) and the three aerodynamic moment coefficients (C_l, C_m, C_n). Each coefficient is a function of angle of attack, sideslip angle, and flap deflection. The longitudinal coefficients (C_x, C_z, C_m) are also a function of elevator deflection and pitch rate, and the lateral-directional coefficients (C_l, C_m, C_n) are also a function of aileron deflection, rudder deflection, roll rate, and yaw rate. The equation form of the nonlinear Twin Otter aerodynamics model is

$$C_Z = C_Z^*(\alpha, \beta) + \Delta C_Z^*(\alpha, \delta_e) + \Delta C_Z^*(\alpha, q) \tag{7}$$

$$C_X = C_X^*(\alpha, \beta) + \Delta C_X^*(\alpha, \delta_e) + \Delta C_X^*(\alpha, q) \tag{8}$$

$$C_m = C_m^*(\alpha, \beta) + \Delta C_m^*(\alpha, \delta_e) + \Delta C_m^*(\alpha, q) \tag{9}$$

$$C_Y = C_Y^*(\alpha, \beta) + \Delta C_Y^*(\alpha, \delta_a) + \Delta C_Y(\alpha, \delta_r) + \Delta C_Y^*(\alpha, p) + \Delta C_Y^\dagger(\alpha, r) \tag{10}$$

$$C_l = C_l^*(\alpha, \beta) + \Delta C_l^*(\alpha, \delta_a) + \Delta C_l(\alpha, \delta_r) + \Delta C_l^*(\alpha, p) + \Delta C_l^\dagger(\alpha, r) \tag{11}$$

$$C_n = C_n^*(\alpha, \beta) + \Delta C_n^*(\alpha, \delta_a) + \Delta C_n(\alpha, \delta_r) + \Delta C_n^*(\alpha, p) + \Delta C_n^\dagger(\alpha, r) \tag{12}$$

The superscript * means that those coefficients are also a function of three flap deflections (0, 20, and 40 deg). The coefficients with a † are a function of two flap deflections (0 and 40 deg).

Autopilot

Because autopilot functions left on during icing conditions can mask the effects of icing on the aircraft flight characteristics, an autopilot was created for the Twin Otter flight model [6]. The current autopilots implemented in the simulator are a pitch attitude hold, an altitude hold, a roll attitude hold, and a heading hold. All of the autopilot routines were developed by the flight controls and sensors group using the Flight Dynamics and Control (FDC) toolbox for Matlab,¶ and the routines were then converted to C functions and integrated in the simulator. The autopilot routines were designed using the linear aerodynamics model of the Twin Otter, but the routines work well within the linear range of the nonlinear aerodynamics model.

¶Data available on-line at http://home.wanadoo.nl/dutchroll/manual.html [cited 3 January 2006].

Table 1 Icing coefficient factors for the longitudinal case of the Twin Otter linear aerodynamics model

	Wing and tail ice	Wing ice	Tail ice
$k_{C_{X_0}}$	6.52696	2.64444	1.58844
$k_{C_{X_\alpha}}$	−0.14296	−0.03156	−0.04504
$k_{C_{X_{\alpha^2}}}$	−1.59837	−0.13719	−0.58415
$k_{C_{Z_\alpha}}$	−1.48148	−0.83259	−0.36593
$k_{C_{Z_q}}$	−0.20741	−0.20741	−0.20741
$k_{C_{Z_{\delta_e}}}$	−1.40741	−0.33970	−1.05556
$k_{C_{m_\alpha}}$	−1.46667	−0.28346	−0.53244
$k_{C_{m_q}}$	−0.51852	−0.51852	−0.51852
$k_{C_{m_{\delta_e}}}$	−1.48148	−0.26504	−1.24756

Simulator Batch Mode

To effectively use the simulator as a testing platform, functionality was added to allow the simulator to run in batch mode. The purpose of the batch mode is to be able to start the simulator at a given initial condition and to be able to control the aircraft through prescribed control inputs. The initial condition of the aircraft is provided through the keyword-based input file by supplying the orientation and velocity. The orientation is given by the three Euler angles while the three body-axis velocities and the three angular rates give the velocity. The position of the aircraft is specified by the altitude, longitude, and latitude provided as command-line options built into FlightGear. Time histories of the control surface and throttle inputs are provided for the simulator as data files. Through the keyword-based input file, one can also provide time histories of the icing parameters, ice protection system values, and envelope protection system values.

Icing Model

Two icing models are used in the IEFS depending on whether a linear or nonlinear aerodynamics model is being used [7]. For the linear aerodynamics model, the icing model uses an icing severity factor η_{ice} and coefficient icing factor $k'_{C_{(A)}}$ to modify the aerodynamic coefficients. The parameter η_{ice} represents the amount and severity of the icing, and it is defined to only be a function of the atmospheric conditions; it is independent of the aircraft. The factor $k'_{C_{(A)}}$ is dependent on the aerodynamic coefficient and on the properties of the aircraft. The resulting iced coefficient is given by

$$C_{(A)_{\text{iced}}} = (1 + \eta_{\text{ice}} k'_{C_{(A)}}) C_{(A)} \tag{13}$$

where $C_{(A)}$ is any aerodynamic coefficient [7]. To model different icing cases, such as wing ice, tail ice, and full aircraft icing, different coefficient icing factors are used (Table 1). The aerodynamics and flight mechanics group used NASA flight test data of a Twin Otter in icing [15–17] to calculate and estimate the coefficient icing factors. These icing factors are meant to be used in all flight conditions and are not a function of flight conditions such as airspeed and angle of attack. This linear model was only used for quasisteady flight analysis [7,8].

For the nonlinear case, the longitudinal iced coefficients are found using an equation similar to the linear icing case [Eq. (13)]. The longitudinal iced coefficients are given by

$$C_{(A)_{\text{iced}}} = (1 + \eta k_{C_{(A)}}) C_{(A)} \tag{14}$$

where η is the aircraft icing parameter and $k_{C_{(A)}}$ is another form of the

coefficient icing factor. The parameter η is similar to η_{ice} except that it is aircraft specific. The relation between $k_{C_{(A)}}$ and $k'_{C_{(A)}}$ is represented by

$$k'_{C_{(A)}} = \frac{\eta}{\eta_{\text{ice}}} k_{C_{(A)}} \tag{15}$$

For the current nonlinear icing model, $k_{C_{(D)}}$ and $k_{C_{(L)}}$ are functions of the angle of attack, and $k_{C_{(m)}}$ is a function of the angle of attack and the elevator deflection. Instead of using Eq. (14) for lateral-directional aerodynamics, the iced rolling moment coefficient $C_{l_{\text{iced}}}$ and the iced yawing moment coefficient $C_{n_{\text{iced}}}$ are a function of the asymmetric lift and drag, respectively, produced by different icing on the left and right sides of the wing.

Both icing factors are provided to the simulator either through the aircraft input file or through the ice weather model. Using the input file method, η_{ice} is modeled by a ramp function, and η is provided in the form of data files that supply a time history of its value. The ice weather model simulates how ice accumulates on the Twin Otter as it passes through a cloud. First the weather model uses the position of the aircraft in the cloud to determine the liquid water content (LWC), cloud drop median volumetric diameter (MVD), and the air temperature. It then passes these values along with the angle of attack, airspeed, and the current values of η_{ice} and η to an ice accretion function to calculate the new values of η_{ice} and η and also the rate of change of η. The ice accretion function was developed to model the icing factors for the wings of a Twin Otter. However, it is also being used to calculate the icing factors of the horizontal tail. This approximate model provides a reasonable value for this first-order ice accretion function.

Ice Management System

Icing Characterization

The core of the ice management system is the neural-network-based icing characterization. This process uses estimates of the flight dynamic parameters and expected values to calculate an estimate of the ice severity [9]. Figure 4 shows the block diagram of the neural-network-based icing characterization routine integrated into the flight simulator. Originally written in Matlab, the neural-network code was converted into C + + using the Matlab 6.0 application program interface (API) [3,18]. It was integrated into the simulator, but the algorithm proved too computationally intensive to estimate η in real time. Because the icing severity is still needed by the other components of the IMS, the true value used by the icing model is provided instead. It will require waiting until the next generation of desktop computers for the icing characterization routine to be fast enough to run in real time.

Envelope Protection System

The envelope protection system was designed to keep the aircraft in a safe flight regime by limiting the angle of attack, pitch angle, roll angle, airspeed, throttle setting, and flap deflection. Conventional envelope protection schemes use predetermined limits on parameters such as angle of attack and bank angle, but this is not always effective in icing situations where the aircraft performance, stability, and control are continuously changing with the ice severity [19]. The EPS designed for the IEFS needs limits calculated in real time. Currently, the EPS calculates the maximum angle of attack (AOA) by estimating the stall angle of attack based on the ice severity. In calculating the maximum AOA, the EPS also finds the maximum lift coefficient. From the maximum AOA and C_L, the maximum pitch angle, minimum throttle setting, and minimum airspeed are determined. To determine the maximum pitch angle, the maximum AOA is added to the steady-state flight path angle. The minimum airspeed is calculated using the maximum C_L found by the EPS and is given by

$$V_{\text{min}} = \sqrt{\frac{2W}{\rho S C_{L_{\text{max}_{\text{iced}}}}}} \tag{16}$$

where W is the weight, ρ is the air density, and S is the wing area. Calculation of the minimum throttle setting is done by estimating the airspeed of the aircraft in the next 10 s. By using the current acceleration of the aircraft, an estimate of the future airspeed is made, and if this estimated airspeed is below the minimum airspeed calculated above, then 10% more throttle than the current setting is given as the minimum throttle setting. If any of the EPS limits are violated, the EPS provides recommended pilot procedures, such as pitch down and throttle up, to correct it. Alerts are given both visually, through the IMS-enhanced glass cockpit, and aurally. It should be noted that the EPS discussed above is a first-order design. The system works well in steady flight or in gentle maneuvers, but the pilot can easily violate the EPS bounds with quick maneuvers.

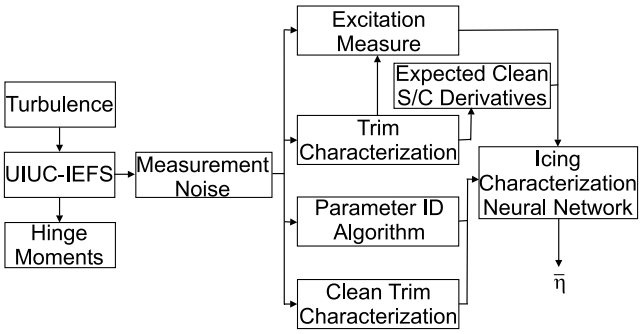

Fig. 4 Neural-network-based icing characterization architecture integrated with the IEFS. The output from the various modules is fed as input to the neural-network block where η estimate is generated.

Ice Protection System

The current ice protection system was modeled by de-ice boots for the left wing, right wing, and horizontal tail. This system allows the pilot to manually control the de-ice boots or have the system controlled by the IMS. When the IPS is in automatic mode, the IMS determines when the de-ice boots should be activated from the sensed ice accretion. Based on the ice accretion rate, the IMS also determines the cycle time of the de-ice boots.

IMS-Enhanced Glass Cockpit

An important goal during the development of the IMS was to be able to present IMS information to the pilot to aid in the decision making process [2,11]. Using the research gathered by the human factors group on pilots' information requirements during icing conditions [20], the IMS-enhanced glass cockpit was designed to inform pilots on the status of the IMS (Fig. 5).** The glass cockpit was developed from baseline software written in OpenGL by Fuesz. In addition to presenting icing data to the pilot, the glass cockpit was also designed to make sure the pilot is aware that new information is being provided. This state of awareness is created with an ambient strip displayed across the glass cockpit to grab the pilot's attention. The strip also leads to and surrounds the specific system to guide the pilot's attention to the problem area (Fig. 6). The ambient strip flashes 3 times then stays illuminated for an additional 10 s.

Icing information from the IMS is provided to the pilot in a variety of ways. The ice severity is presented to the pilot on a bird's eye view of the aircraft showing its location, and the pilot is also informed aurally. There are four levels of icing that are presented to the pilot: light, moderate, severe, and no ice detected. Figure 7 shows the ice levels displayed to the pilot. Light icing is shown as blue on the bird's eye view of the aircraft, and a yellow ambient strip is used. Moderate icing is shown as yellow, and a yellow ambient strip is again used. Severe icing is shown as red, and a red ambient strip is used. When icing is no longer detected, the bird's eye view is clear, and a blue

**For color versions of the figures see http://www.ae.uiuc.edu/m-selig/apasim/pubs/.

ambient strip is used. For the light, moderate, and severe icing cases, an auditory warning is also provided.

Limits provided by the EPS are displayed on the electronic attitude director indicator (EADI), throttle indicator, airspeed indicator, angle of attack indicator, and flap indicator. The EADI displays both the pitch and the roll limits. When the aircraft reaches or passes the indicated limits, the EPS informs the pilot that the limit has been reached and may also provide a recommended procedure. The glass cockpit indicators include color to inform the pilot of EPS limits. Values beyond these limits are indicated in red. Examples include pitch and roll angles greater than the EPS maximums, flap positions greater than the EPS maximum, throttle settings lower than the EPS minimum, and airspeeds lower than the EPS minimum. Exceeding the maximum roll angle causes the roll indicator to turn red (Fig. 8). The flap indicator also turns red if its limit is reached (Fig. 9). Throttling down below the minimum throttle setting causes the throttle indicator to turn red and to provide a throttle up command to the pilot (Fig. 10). Three limits trigger a pitch down command from the flight director on the EADI: maximum pitch angle, maximum angle of attack, and minimum airspeed (Fig. 11). The angle of attack indicator is color coded to better inform the pilot of the aircraft state. The indicator is green from 0 to 40%, yellow from 40 to 80%, and red from 80 to 100% of the maximum angle of attack. A pitch up command is also provided when the minimum pitch angle is reached (Fig. 12).

The final information the glass cockpit provides to the pilot is the status of the de-ice boots. Status bars of the three de-ice boots inform the pilot at what level the boots are currently set (Fig. 13). If a boot were to fail, the glass cockpit would also provide this information by turning that particular boot indicator red and using a red ambient strip to grab the pilot's attention (Fig. 14).

Fig. 5 Glass cockpit display and IMS interface.

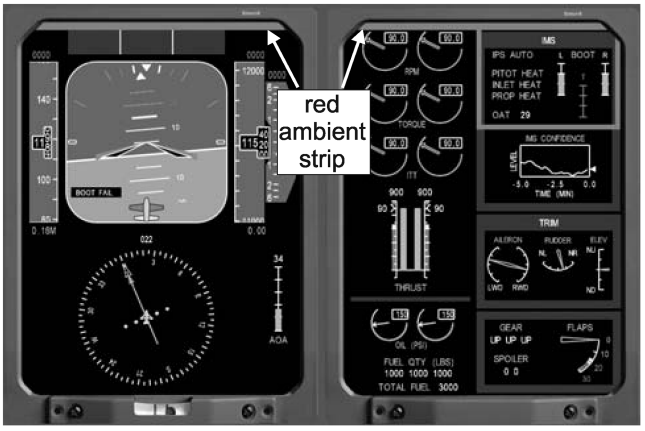

Fig. 6 Ambient strip (red) showing boot failure.

Distributed Simulation

The Icing Encounter Flight Simulator contains several processor-intensive modules, which include the flight dynamics model, an out-the-window display, the glass cockpit display, and the neural-network-based icing characterization. Whereas a modern Pentium-

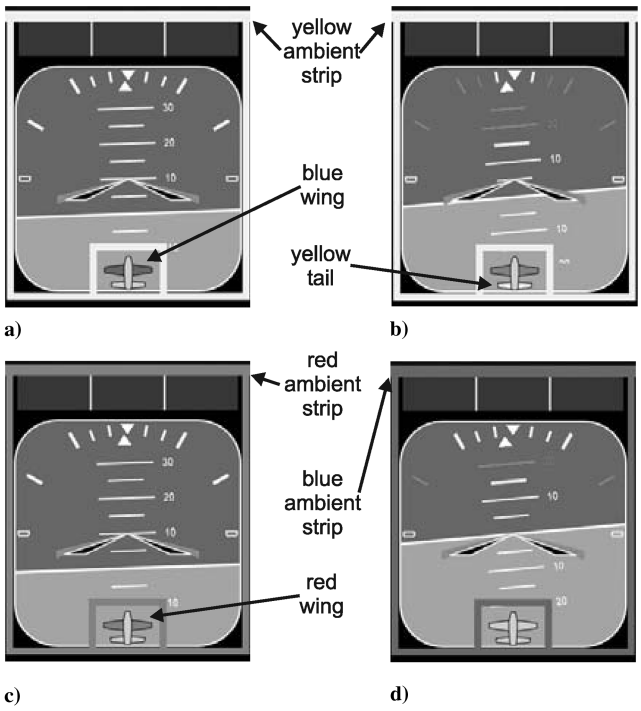

Fig. 7 Four levels of ice severity displayed to the pilot: a) light icing on the wing (blue) with yellow ambient strip, b) moderate icing on the tail (yellow) with yellow ambient strip, c) severe icing on the wing (red) with red ambient strip, d) ice no longer detected with blue ambient strip.

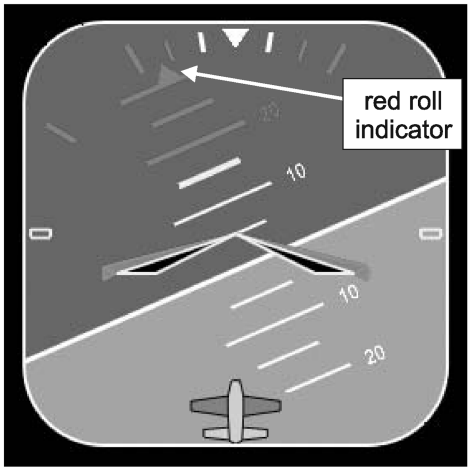

Fig. 8 Roll angles greater than the EPS maximum are red, and the roll indicator is red because the maximum roll angle is exceeded.

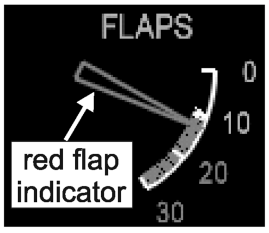

Fig. 9 Flap positions greater than the EPS maximum are red, and the flap indicator is red because the maximum flap position is exceeded.

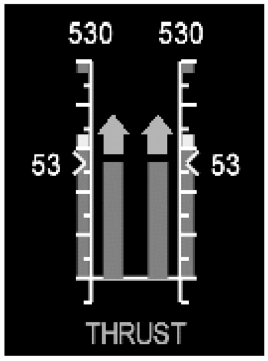

Fig. 10 Throttle settings lower than the EPS minimum are red, and an increase throttle command is given (green arrow up) because the throttle setting is below the EPS minimum throttle.

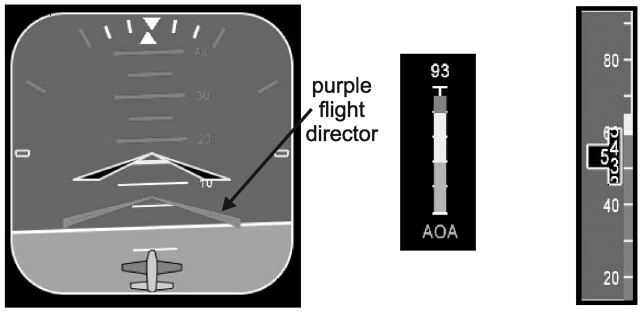

a) b) c)

Fig. 11 Pitch down command shown by the flight director (purple) since a) maximum pitch angle reached, b) maximum angle of attack is reached, or c) minimum airspeed is reached.

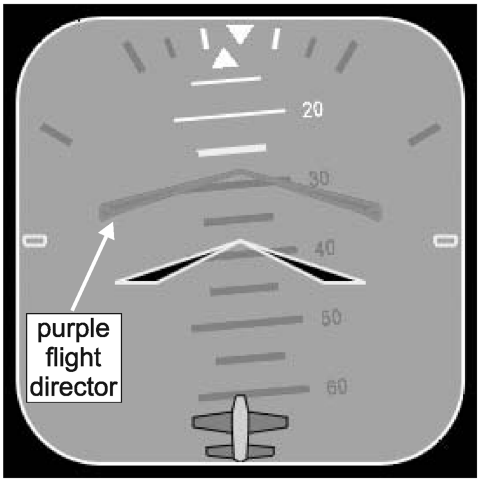

Fig. 12 Pitch up command given by the flight director (purple) since the minimum pitch angle is reached.

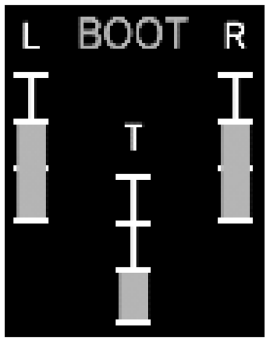

Fig. 13 De-ice boots status display. Wing de-ice boots are on medium, and tail de-ice boot is on low.

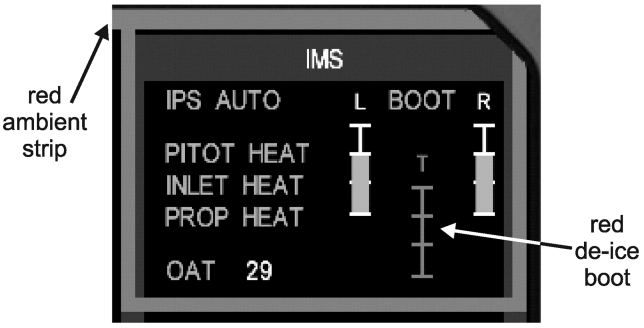

Fig. 14 Failed tail de-ice boot (red) with red ambient strip.

based PC is capable of executing one or two of these modules concurrently, a complete simulation requires the use of multiple processors for real-time, parallel execution of all modules. To this end, the simulation runs across multiple PCs (up to nine in total), each handling one or more modules. Note that the icing characterization module still cannot be run in real time on a dedicated processor, but this limitation is expected to be overcome as faster processors are released. The distributed approach to computationally demanding tasks has long been used in commercial flight simulators and myriad other systems where discrete-time events may be processed independently.

The IEFS distributed model combines a client-server architecture with some peer-to-peer features for increased performance. A central server maintains the master simulation state and communicates with each of the clients using the Transmission Control Protocol/Internet Protocol (TCP/IP) in a networked environment. The clients, in turn, host the simulator modules, with each module running in a separate process. One machine may host several modules, although processor-intensive modules are run on dedicated PCs for practical real-time execution. A top-level IEFS communication protocol is derived from the sockets API, providing library functions for simple input/output (I/O) in each client [21].

During one simulation time step, each module receives a relevant subset of the current simulation state via the IEFS protocol, performs module-specific state updates, and transmits the new state subset to the server. To alleviate some issues regarding the order in which state variables are read and updated, state variables can be broadcast simultaneously to all clients in peer-to-peer fashion when necessary, instead of passing through the server for distribution. Most variables, however, are not as time sensitive and are only used by a few clients, making them better candidates for the client-server method [22].

Real-time simulation was necessary for this project to have the capability of testing and demonstrating the IMS with a pilot in the loop. Because of this real-time need, a simulator time step was selected that would still allow the simulator to run in real time. The real-time dynamics were run at 120 Hz. Visuals were updated at 30 Hz to have smooth animation. State variables such as aircraft location and velocity were calculated by the FDM and broadcasted to the other modules at 30 Hz, a rate adequate for pilot-in-the-loop feedback.

Icing Encounter Scenarios with the IEFS

The Icing Encounter Flight Simulator is designed to integrate all SIS component functions and demonstrate their effectiveness in a simulated icing environment. For this purpose, two scenarios were developed to simulate potentially dangerous icing encounters in commuter aircraft. The majority of serious in-flight icing encounters may be categorized as either roll upset or tailplane stall events [23–25], each of which is represented by one of the scenarios. Although fictional, these icing encounter scenarios include elements of real-world incidents and accidents, showcasing the potential of the IMS to prevent icing related accidents through various interventions. Real-world accidents typically result from a chain of unlikely and unfortunate events, each a necessary component in the final result [12]. The fictional scenarios were built on this premise, allowing the IMS

Table 2 Common contributing factors to in-flight icing events

Excessive loitering in large-droplet icing conditions
Ice accumulation behind de-ice boots
Aircraft inadequately equipped for large-droplet conditions
Pilots unaware of icing severity due to inadequate sensors and/or lack of pertinent weather information
Wing and/or tail at high angle of attack
Autopilot engaged during known icing conditions
Inoperative de-ice or anti-ice equipment
Failure to use available de-ice and anti-ice equipment
Atmospheric temperature inversion during approach phase
Use of flaps

to eliminate the icing threat by intervening at one of many possible points in the event chain.

Historical Factors

A review of U.S. in-flight icing events over the past 20 years has revealed an extensive list of contributing factors. Specific events and individual factors are not listed here, but a list of common factors is given in Table 2.

As mentioned earlier, any one of these factors is normally insufficient to cause an icing event. Instead, three or more factors typically combine to produce a series of failures in the three lines of conventional icing defense: avoidance, IPS, and the pilot [1,12]. The tailplane stall and roll upset scenarios presented here cast the IMS as an extra layer of protection in icing defense, reducing the risk of multiple factors combining to produce an event. As previously discussed, Fig. 2 conceptually illustrates this extra line of defense. As an event chain passes through weaknesses in the three conventional layers of defense, it is stopped by the new IMS layer. Each scenario refers to a conventional aircraft without an IMS, but possible IMS intervention points are given throughout. Each hypothetical intervention is understood to be capable of breaking the icing event chain.

Tailplane Stall

The first icing scenario depicts a tailplane stall, which is caused when ice contaminates the leading edge of the horizontal tailplane. This event usually occurs when flaps have been deployed causing an increase of downwash on the tail. The ice and increased downwash cause turbulent or separated flow on the tailplane, which in turn results in the elevator hinge moment being reduced or reversed or having the tailplane completely stall. Since flaps are usually extended during final approach to land, a tailplane stall can lead to a deadly accident due to the proximity to the ground [26].

In the fictional tailplane stall scenario, a 40-passenger commuter turboprop is considered on approach to a mountainous airport in icing conditions. The aircraft is operating near the edge of its certified flight envelope with a full passenger load and forward center of gravity (CG). To add to the pilot workload, the scenario involves a runway change during the approach phase, as well as an unidentified hydraulic problem. Furthermore, the weather reports over the destination provide an incomplete picture of the quality and location of icing conditions.

The tailplane stall event scenario sequence is illustrated in Fig. 15. The initial descent (1) and approach (2) proceed normally until a runway change is issued because of changing wind conditions (3). At this point, the crew begin maneuvering for a new approach and become preoccupied with the tasks associated with this change. Around the same time, the aircraft enters icing conditions and begins accreting glaze ice (4). Distracted by the new approach, the crew are not immediately aware of the developing icing situation.

IMS intervention: pilot notification. As ice accumulates on the aircraft, traditional icing probes as well as the icing characterization system, through the effects of ice on aircraft dynamics, would detect the presence of ice. The pilots would be notified of the possibility of ice through visual and auditory cues. Visually, a small icon of an aircraft would be displayed on the glass cockpit with the possible location of the icing. An ambient strip would flash and surround the aircraft icon to capture the crew's attention (Fig. 16). An auditory warning such as "tail icing likely" would also be provided for addition emphasis.

IMS intervention: IPS activation. Upon detecting airframe icing, the IMS would automatically activate conventional IPS devices such as de-ice boots and pitot heat.

The crew, following standard procedure, notice ice buildup on the windshield wipers after several minutes in icing conditions. They immediately activate anti-ice devices and start the de-ice boots on a 3 min cycle (5). Shortly thereafter, the cockpit workload is further increased by the illumination of a master hydraulic warning light. No handling problems are observed, and the crew continue to fly the new approach while working the hydraulic problem. Shortly before turning final, the tail de-ice boot fails to deploy (6). A small warning light is displayed on the panel, but the crew's attention is dominated by the hydraulic situation and the approach.

IMS intervention: pilot notification. The IMS-enhanced glass cockpit employs an attention-grabbing ambient strip to alert pilots to failures and critical warnings (Fig. 17). Such a feature would be used to alert the scenario crew to the de-ice boot failure, prompting a more conservative approach angle.

Unaware of the boot failure, the crew intercept the localizer (7) and begin the unusually steep final approach for this mountain runway. Several minutes later, full flaps are deployed (8), followed shortly thereafter by a loss of longitudinal control due to tailplane stall (9).

IMS intervention: envelope protection. The envelope protection system would alert the pilots to the initial unsafe descent attitude as

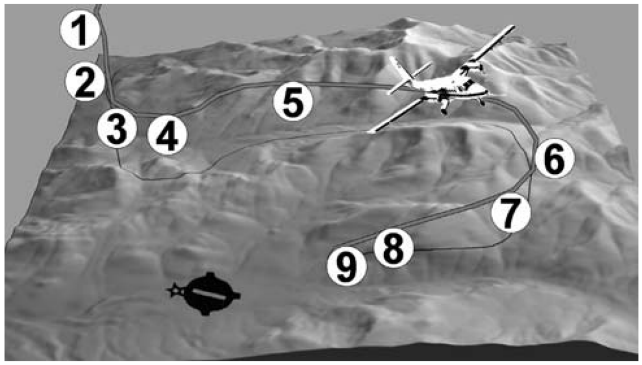

Fig. 15 Tailplane stall event sequence: 1) initial descent, 2) initial approach, 3) runway change, 4) ice accretion begins, 5) IPS activated, 6) tail de-ice boot fails, 7) localizer intercepted, 8) full flaps deployed, and 9) tailplane stall.

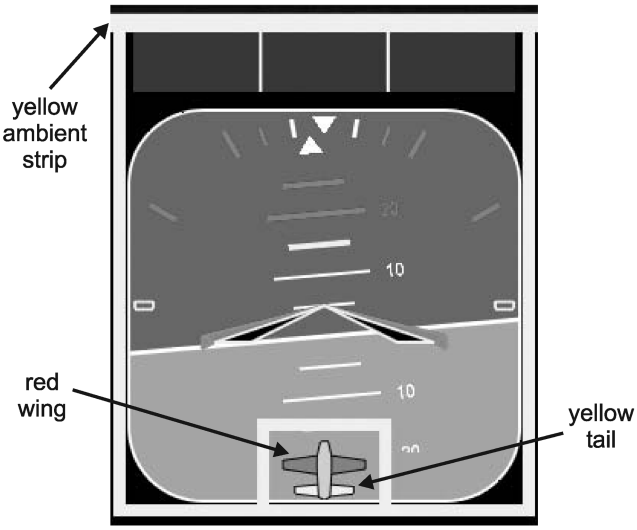

Fig. 16 Ice accretion notification with severe wing ice (red) and moderate tail ice (yellow) shown. The ambient strip (yellow) flashes and surrounds the aircraft icon to capture the attention of the pilot.

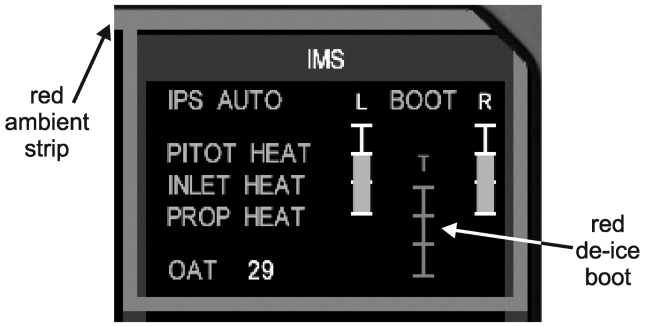

Fig. 17 Red ambient strip warning for failed tail de-ice boot (tail indicator red).

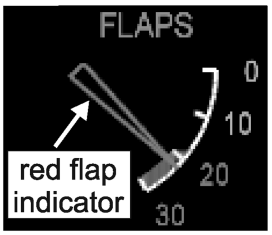

Fig. 18 Envelope protection warning that maximum flap angle exceeded (flap indicator red).

well as the maximum safe flap extension dictated by the tailplane icing. Either intervention would prevent the high tail force that leads to the tailplane stall. Figure 18 shows the EPS warning for the maximum flap extension.

Roll Upset

The second icing scenario involves a roll upset, which is a severe rolling moment caused by separation in front of the ailerons, leading to uncommanded deflections of unpowered ailerons. A roll upset is often the result of ice accumulation behind the de-ice boots [27]. This scenario occurs at night in icing conditions when a 40-passenger commuter aircraft returns to the departure field following an engine failure. As in the first scenario, the crew are provided with an inadequate icing report before departure, and a high degree of Air Traffic Control (ATC) vectoring adds to the cockpit workload. In addition, the aircraft ultrasonic icing probe is inoperative, unbeknownst to the crew. As in the tailplane stall scenario, the roll upset scenario refers to a conventional aircraft without an IMS, but possible IMS intervention points are given throughout. Each hypothetical intervention is understood to be capable of breaking the icing event chain.

The roll upset scenario event sequence is illustrated in Fig. 19. As the scenario unfolds, the aircraft departs 30 min late (1) and is quickly bombarded with ATC requests during an especially busy night in a major class-B airspace (2). During climbout, the crew observes abnormal temperature and oil pressure readings on the right engine (3) and immediately focuses attention on this issue. Anti-ice measures are activated as they climb through known icing conditions, but the inoperative icing probe fails to detect significant rime ice buildup on the main wings (4). The crew, distracted by the engine issue and ATC requests, does not place high priority on monitoring the icing status, instead relying upon the failed probe.

IMS intervention: pilot notification. Even though the ice probe has failed, the presence of ice would be detected by the icing characterization system due to the changes in aircraft dynamics. The pilots would be notified of the possibility of ice through visual and auditory cues. Visually, a small icon of an aircraft would be displayed on the glass cockpit with the possible location of the icing. An ambient strip would flash and surround the aircraft icon (Fig. 20). An auditory warning such as "wing icing likely" would also be provided for addition emphasis.

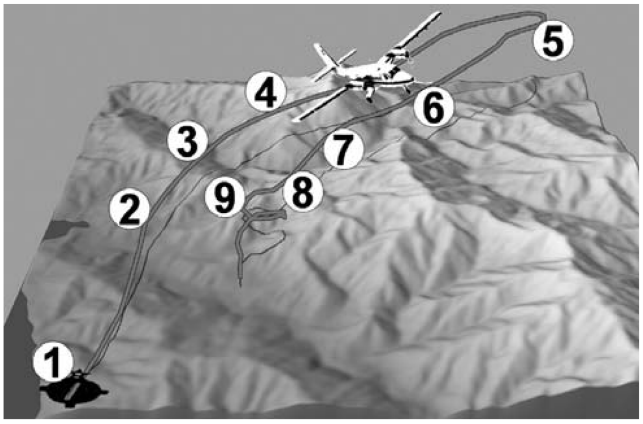

Fig. 19 Roll upset event sequence: 1) aircraft departs, 2) bombarded with ATC requests, 3) abnormal right engine readings, 4) anti-ice measures activated, ice probe fails, and rime ice buildup on the main wings, 5) heads back to point of origin, 6) right engine fails, 7) full flaps deployed and airspeed reduced, 8) de-ice boots activated, and 9) two roll excursion events.

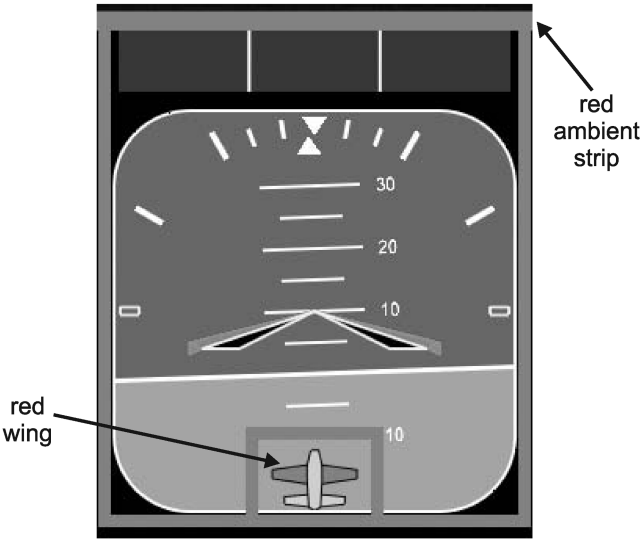

Fig. 20 Ice accretion notification with severe wing ice (red) shown. The ambient strip (red) flashes and surrounds the aircraft icon to capture the attention of the pilot.

IMS intervention: IPS activation. Upon detecting airframe icing, the IMS would automatically activate conventional IPS devices such as de-ice boots and pitot heat.

As the engine problem worsens, the crew experience handling difficulties and elect to return to the point of origin (5). Still unaware of the growing ice accretion on the main wings, they attribute the handling problems to a loss of hydraulic pressure related to the engine problem. The right engine soon fails altogether, prompting the crew to declare an emergency and request priority vectoring to the airfield (6). As the aircraft approaches the final approach, flaps are deployed, and the airspeed is reduced (7). Soon after, the crew notice clear ice buildup on a nose-mounted probe, prompting them to activate the de-ice boots (8). Unfortunately, some aft wing ice remains following the late deployment of leading-edge boots, leading to severe flow problems on the main wings. Loss of lateral control occurs almost immediately, causing two roll excursion events (9).

IMS intervention: envelope protection. Sensing the diminished handling qualities caused by partial wing ice following the late activation of de-ice boots, the envelope protection system would issue angle of attack and pitch attitude alerts, discouraging the crew from placing the aircraft in an unsafe attitude during approach. Figure 21 shows an angle of attack gauge indicating an angle near the

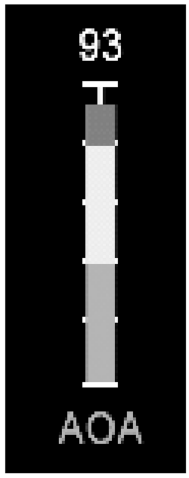

Fig. 21 Envelope protection warning that angle of attack is approaching limit.

Fig. 22 Envelope protection warning that aircraft is nearing unsafe attitude (pitch down command).

imposed limit. Figure 22 shows the pitch down command given when an unsafe attitude is reached.

IEFS Implementation

Two different IEFS setups were used to demonstrate the icing scenarios. The first setup was used for testing purposes and uses four desktop PCs whereas the second setup uses nine PCs and was used to demonstrate the full potential of the IEFS. The second setup was also filmed to create a digital versatile disc (DVD) to explain and demonstrate the SIS project for NASA [28]. Two Linux-based PCs and two Windows-based PCs make up the basis of the first IEFS setup (Fig. 23). One Linux PC was used as the server to maintain the master state of the simulation. This PC also ran a manual state controller which allowed the user to manually change simulation states using a web page-based interface. The second Linux PC ran two modules: the flight dynamics model from FlightGear and the SIS support codes. Both Windows machines were used for visuals. The first ran the IMS-enhanced glass cockpit, and the second ran the out-the-window view using Microsoft Flight Simulator 2002. The glass cockpit computer also read input from a joystick for control surface and throttle deflections and sent that data to the server to be used by FlightGear. Linux PCs were used for FlightGear and the server because these programs run faster on the Linux platform. The glass cockpit was on a Windows-based PC to take advantage of Windows-based graphics. The manual state controller is run on a Linux or Windows PC depending on which type of PC is available.

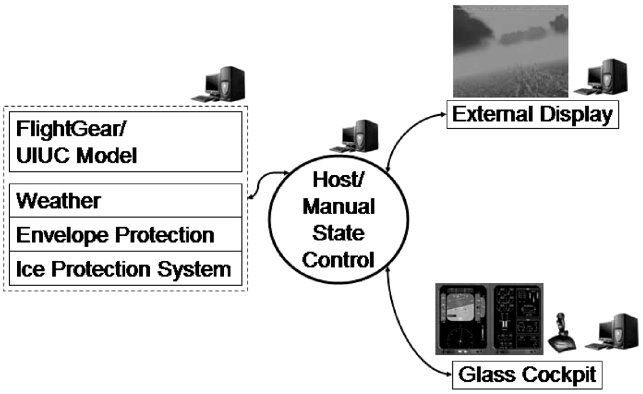

Fig. 23 IEFS layout used for testing purposes.

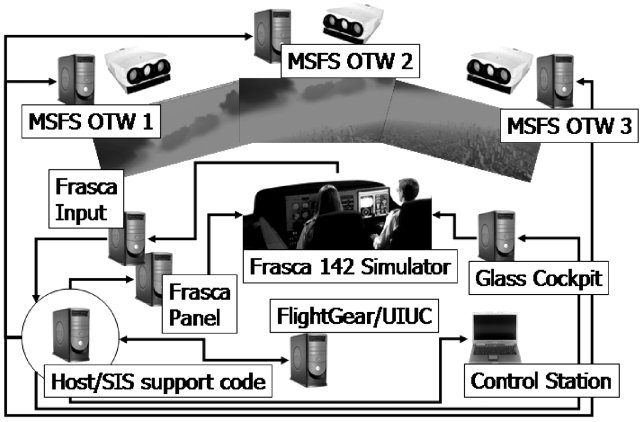

Fig. 24 IEFS layout used for demonstration purposes.

The second IEFS setup was more complicated (Fig. 24). Instead of flying the simulator through a joystick at a PC like the first setup, a Frasca 142 Simulator was used for control inputs. Using the Frasca simulator added two more computers: one to receive control inputs from the Frasca 142 and the other to send data to the Frasca 142 panel so that the pilots would see accurate simulation data on their gauges. Again one Windows PC was used for the IMS-enhanced glass cockpit, but three Windows PCs running Microsoft Flight Simulator 2002 were used for the out-the-window views. Three out-the-window view PCs were used to add peripheral cues for the pilots. Two Linux machines were used in this setup. One ran the server and the SIS support codes whereas the other ran FlightGear for the flight dynamics model. The last computer in the setup was a laptop running Windows for the manual state controller.

Summary

The Icing Encounter Flight Simulator is the systems integrator for the Smart Icing Systems Research Group. The simulator incorporates the icing model, the ice management system, and the IMS-enhanced glass cockpit. The purpose of the IMS is to improve the safety of the aircraft in icing conditions by sensing and characterizing ice accretion, notifying the pilot, and if necessary taking measures to ensure the safety of the aircraft. Components of the IMS include the icing characterization neural network to sense ice accretion, the envelope protection system to keep the aircraft in a safe flight envelope, and the ice protection system to activate de-ice boots and de-icing equipment. Other components of the IEFS include the reconfigurable aircraft model, autopilot, and batch mode, which were all added to the FlightGear flight simulator. The IEFS modules were run on several networked computers to ensure real-time simulation. Two fictional but historically motivated icing scenarios were used with the IEFS to evaluate the effectiveness of the IMS. These scenarios were modeled after two of the most dangerous types of in-

flight icing encounters: tailplane stall and roll upset. In both of the scenarios, distractions and undetected ice accretion lead to the eventual loss of control of a conventional aircraft without an IMS. During each scenario, numerous IMS intervention points are suggested. Any intervention is understood to break the chain of events leading to a catastrophic icing event.

Acknowledgments

This research has been sponsored by NASA Glenn Research Center, and its support is gratefully acknowledged. The authors wish to acknowledge Bipin Sehgal and Jeff Scott (both former UIUC AAE graduate students) for their valuable contributions to the IEFS code. Appreciation and thanks goes to Brian Fuesz for his initial work on the glass cockpit and to the SIS Research Group for all of their contributions. Also, the FlightGear development group is thanked for all their help, support, and suggestions.

References

[1] Bragg, M. B., Perkins, W. R., Sarter, N. B., Basar, T., Voulgaris, P. G., Gurbacki, H. M., Melody, J. W., and McCray, S. A., "An Interdisciplinary Approach to Inflight Aircraft Icing Safety," AIAA Paper 98-0095, Jan. 1998.

[2] Bragg, M. B., Perkins, W. R., Basar, B., Voulgaris, P. G., Selig, M. S., Melody, J. W., and Sarter N. B., "Smart Icing Systems for Aircraft Icing Safety," AIAA Paper 2002-0813, Jan. 2002.

[3] Sehgal, B., Deters, R. W., and Selig, M.S., "Icing Encounter Flight Simulator," AIAA Paper 2002-0817, Jan. 2002.

[4] Deters, R. W., Dimock, G.A., and Selig, M.S., "Icing Encounter Flight Simulator with an Integrated Smart Icing System," AIAA Paper 2002-4599, Aug. 2002.

[5] Dimock, G. A., Deters, R. W., and Selig, M. S., "Icing Scenarios with the Icing Encounter Flight Simulator," AIAA Paper 2003-0023, Jan. 2003.

[6] Sharma, V., and Voulgaris, P., "Effects of Ice Accretion on Aircraft Autopilot Stability and Performance," AIAA Paper 2002-0815, Jan. 2002.

[7] Bragg, M. B., Hutchison, T., Merret, J., Oltman, R., and Pokhariyal, D., "Effects of Ice Accretion on Aircraft Flight Dynamics," AIAA Paper 2000-0360, Jan. 2000.

[8] Pokhariyal, D., Bragg, M. B., Hutchison, T., and Merret, J., "Aircraft Flight Dynamics with Simulated Ice Accretion," AIAA Paper 2001-0541, Jan. 2001.

[9] Melody, J. W., Pokhariyal, D., Merret, J., Basar, T., Perkins, W. R., and Bragg, M. B., "Sensor Integration for Inflight Icing Characterization Using Neural Networks," AIAA Paper 2001-0542, Jan. 2001.

[10] Hossain, K., Sharma, V., Bragg, M. B., and Voulgaris, P.G., "Envelope Protection and Control Adaptation in Icing Encounters," AIAA Paper 2003-0025, Jan. 2003.

[11] Sarter, N. B., and Schroeder, B. O., "Supporting Decision-Making and Action Selection Under Time Pressure and Uncertainty: The Case of Inflight Icing," *Human Factors* (to be published).

[12] Maurino, D. E., Reason, J., Johnston, N., and Lee, R. L., *Beyond Aviation Human Factors*, Avebury Aviation, Hants, U.K., 1995.

[13] Jackson, E. B., "Manual for a Workstation-Based Generic Flight Simulation Program (LaRCsim) Version 1.4," NASA TM 110164, April 1995.

[14] Deters, R. W., "Icing Encounter Flight Simulator with an Integrated Smart Icing System," M.S. Thesis, University of Illinois at Urbana–Champaign, Urbana, IL, 2003.

[15] Ranaudo, R. J., Batterson, J. G., Reehorst, A. L., Bond, T. H., and O'Mara, T. M., "Determination of Longitudinal Aerodynamic Derivatives Using Flight Data from an Icing Research Aircraft," NASA TM 101427, Jan. 1989; also AIAA Paper 89-0754.

[16] Ratvasky, T. P., and Ranaudo, R. J., "Icing Effects on Aircraft Stablility and Control Determined from Flight Data," NASA TM 105977, Jan. 1993; also AIAA Paper 93-0398.

[17] Ranaudo, R. J., Mikkelsen, K. L., McKnight, R. C., Ide, R. F., Reehorst, A. L., Jordan, J. L., Schinstock, W. C., and Platz, S. J., "The Measurement of Aircraft Performance and Stability and Control After Flight Through Natural Icing Conditions," AIAA Paper 86-9758, April 1986.

[18] Sehgal, B., "Icing Encounter Flight Simulator," M.S. Thesis, University of Illinois at Urbana–Champaign, Urbana, IL, 2002.

[19] Merret, J., Hossain, K., and Bragg, M. B., "Envelope Protection and Atmospheric Disturbances in Icing Encounters," AIAA Paper 2002-0814, Jan. 2002.

[20] McGuirl, J. M., and Sarter, N. B., "Inflight Icing: A Survey of Regional Carrier Pilots," CSEL Technical Report prepared for NASA Glenn Research Center, Columbus, OH, The Ohio State University, 2001 (unpublished).

[21] Stevens, R. W., *Unix Network Programming*, Vol. 1, Prentice–Hall, Inc., Upper Saddle River, NJ, 1998.

[22] Fujimoto, R. M., *Parallel and Distributed Simulation Systems*, Wiley, New York, 2000.

[23] National Transportations Safety Board, "Aircraft Accident Report: Unstabilized Approach and Loss of Control, NPA, Inc. d.b.a. United Express Flight 2415, British Aerospace BA-3101, N41OUE, Tri-Cities Airport, Pasco, Washington, Dec. 26, 1989," National Transportation Safety Board, PB91-910406, NTSB/AAR-91/06, Washington, D.C., 1990, 62 pages.

[24] National Transportations Safety Board, "Aircraft Accident Report: In-Flight Icing Encounter and Loss of Control, Simmons Airlines, d.b.a. American Eagle Flight 4184, Avions de Transport Regional (ATR), Model 72-212, N401AM, Roselawn, Indiana, Oct. 31, 1994, Volume 1: Safety Board Report," National Transportation Safety Board, PB96-910401, NTSB/AAR-96/01, DCA95MA001, Washington, D.C., 1990, 322 page.

[25] National Transportations Safety Board, "Aircraft Accident Report: In-Flight Icing Encounter and Loss of Control, Simmons Airlines, d.b.a. American Eagle Flight 4184, Avions de Transport Regional (ATR), Model 72-212, N401AM, Roselawn, Indiana, Oct. 31, 1994, Volume 2: Response of Bureau Enquetes—Accidents to Safety Board's Draft Report," National Transportation Safety Board, PB96-910402, NTSB/AAR-96/02, DCA95MA001, Washington, D.C., 1990, 274 pages.

[26] Federal Aviation Administration, "Ice Contaminated Tailplane Stall (ICTS)," Advisory Circular 23.143-1, Dec. 2001.

[27] Transport Canada, "Airborne Icing Ground/Flight Training Programmes," Commercial and Business Aviation Advisory Circulars: Guidance Material S742.76(21), S743.98(268), S744.115(31), S745.124(40), April 2003.

[28] UIUC Smart Icing Systems Research Group, Smart Icing Systems, DVD video, produced by NASA Glenn Research Center, Icing Branch, Cleveland, OH, 2003.